Long range p-wave proximity effect into a disordered metal

Aydin Cem Keser, Valentin Stanev, and Victor Galitski

Phys. Rev. B **91**, 094518 — Published 30 March 2015

DOI: 10.1103/PhysRevB.91.094518

Long range p-wave proximity effect into a disordered metal

Aydin Cem Keser,[1] Valentin Stanev,[1] and Victor Galitski[2,3]

[1] *Condensed Matter Theory Center, Department of Physics, University of Maryland, College Park, MD 20742-4111, USA*

[2] *Joint Quantum Institute and Condensed Matter Theory Center, Department of Physics, University of Maryland, College Park, MD 20742-4111, USA*

[3] *School of Physics, Monash University, Melbourne, Victoria 3800, Australia*

(Dated: February 27, 2015)

We use quasiclassical methods of superconductivity to study the superconducting proximity effect from a topological p-wave superconductor into a disordered quasi-one-dimensional metallic wire. We demonstrate that the corresponding Eilenberger equations with disorder reduce to a closed non-linear equation for the superconducting component of the matrix Green's function. Remarkably, this equation is formally equivalent to a classical mechanical system (i.e., Newton's equations), with the Green function corresponding to a coordinate of a fictitious particle and the coordinate along the wire corresponding to time. This mapping allows us to obtain exact solutions in the disordered nanowire in terms of elliptic functions. A surprising result that comes out of this solution is that the p-wave superconductivity proximity-induced into the disordered metal remains long-range, decaying as slowly as the conventional s-wave superconductivity. It is also shown that impurity scattering leads to the appearance of a zero-energy peak.

I. INTRODUCTION

Superconducting heterostructures have attracted a lot of attention recently as possible hosts of Majorana fermions[1–9]. One of the important outstanding questions in the studies of these heterostructures is the interplay between topological superconductivity and disorder[10–13]. Here we explore this issue focusing on the leakage of p-wave superconductivity into a disordered metal. Naïvely, it may not appear to be a particularly meaningful question, because unconventional superconductivity is known to be suppressed by disorder per Anderson's theorem[14]. However, Anderson's theorem is only relevant to an intrinsic superconductor and has little to do with a leakage of superconductivity.

The linearized Usadel equations are standard tools in studies of proximity effects[15,16]. Their derivation, however, assumes that an anisotropic component of the superconducting condensate's wave-function is small compared to the isotropic one, which is not the case in the systems we are interested in. Here, we focus on the more general Eilenberger equations[17,18], which allow us to straightforwardly model systems with complicated geometries, and varying degree of disorder. (In the context of topological superconductivity, similar approach has been used in Refs. 19–22.)

In this work, we consider an infinite quasi-one-dimensional system (nanowire), at least part of which is superconducting. To describe the electronic correlations in the system we utilize the quasiclassical Green's function $\hat{g}$ – a matrix in Nambu and spin space[18]. It is obtained from the full microscopic Green's function, and faithfully captures the long length scale features of the system[23]. In a one-dimensional model, $\hat{g}$ depends on the Matsubara frequency (ω), the center-of-mass coordinate of the pair (x), and the direction of the momentum at the Fermi points ($\zeta \equiv \mathbf{p}_x/p_F$ is $+1/-1$ for right/left going particles). It obeys the Eilenberger equation[16–18]

$$\zeta v_F \partial_x \hat{g} = -[\omega\hat{\tau}_3, \hat{g}] + i[\hat{\Delta}, \hat{g}] - \frac{1}{2\tau_{imp}}[\langle\hat{g}\rangle, \hat{g}]. \quad (1)$$

Here $\hat{\tau}$ are the Pauli matrices in Nambu space. The effects of impurities enter the equation through the last term, in which τ_{imp} is the mean time between collisions, and $\langle ...\rangle$ denotes an average over the Fermi surface (actually, two disconnected points in the one-dimensional case). Since we are interested in wires in which superconductivity is induced by a proximity with a bulk superconductor, we treat $\hat{\Delta}$ as an external parameter, which, furthermore, we assume constant throughout the wire. This allows us to ignore self-consistency, and simplifies the calculations.

The outline of this paper is as follows. In Sec. II and Sec. III, we obtain exact solutions of Eq. (1) for s-wave and p-wave order parameters respectively. In Sec. IV we introduce an intuitive picture for the behavior of the solution by mapping the equations to the equation of motion of a classical particle in an external force field. In Sec. V we study superconducting correlations induced by proximity in a metallic wire. In particular, we demonstrate that the p-wave correlations can be surprisingly long-ranged, even in the presence of disorder. We also show that impurity scattering produces a zero-energy peak in the density of states (DOS). We summarize the results of our work in Sec VI. Although self-consistency is not relevant for the experimental setup we are considering, in the Appendix we provide for completeness the solutions of the fully self-consistent Eilenberger equations for both s-wave and p-wave quasi-one-dimensional superconductors.

II. THE S-WAVE CASE

We decompose $\hat{g}$ in Nambu space using the Pauli matrices τ_i: $\hat{g} = -ig_1\hat{\tau}_1 + g_2\hat{\tau}_2 + g_3\hat{\tau}_3$. The off-diagonal scalar functions g_1 and g_2 describe the superconducting particle-particle correlations, whereas the diagonal component g_3 contains the particle-hole correlations. These functions have to satisfy the normalization condition $-g_1^2 + g_2^2 + g_3^2 = 1$.

In the case of an s-wave superconductor, $\hat{\Delta}$ is a spin-singlet and, ignoring the spin indices, it can be written as $\Delta_0 i\tau_2$ – this is equivalent to choosing the order parameter to be purely real. We ignore self consistency and assume that Δ is constant in space. The function g_2 is in the same channel as $\hat{\Delta}$, and thus encodes the s-wave pairing correlations. The g_1 function has more interesting origin – it describes the p-wave, odd-frequency superconducting correlations, induced by boundaries or other inhomogeneities, and disappearing in bulk uniform superconductors [24–27]. The component g_1 is odd in momentum, therefore its Fermi surface average vanishes identically $\langle g_1 \rangle = 0$. The components g_2 and g_3 are even in momentum, therefore $\langle g_2 \rangle = g_2$ and $\langle g_3 \rangle = g_3$ are satisfied. With these considerations, Eq. 1 can be now written as a set of three coupled first order differential equations for the scalar functions g_i:

$$\zeta v_F \partial_x g_1 = -2\omega g_2 + 2\Delta g_3, \tag{2a}$$

$$\zeta v_F \partial_x g_2 = -2\omega g_1 - \frac{1}{\tau_{imp}} g_1 g_3, \tag{2b}$$

$$\zeta v_F \partial_x g_3 = 2\Delta g_1 + \frac{1}{\tau_{imp}} g_1 g_2. \tag{2c}$$

To be integrable this system of equations has to have two constants of integration. The norm of $\hat{g}$, which is $-g_1^2 + g_2^2 + g^3 = 1$ is one of them. We have identified another constant C_s, given by

$$C_s = g_1^2/(2\tau_{imp}) + 2\Delta g_2 + 2\omega g_3, \tag{3}$$

and obeying $\partial_x C_s = 0$. Note that the value of C_s can be fixed using the appropriate boundary conditions. Using it we can reduce the system given by Eq. (2) to a single second order differential equation for g_1:

$$v_F^2 \partial_x^2 g_1 = \left(4\omega^2 + 4\Delta^2 + \frac{C_s}{\tau_{imp}}\right) g_1 - \frac{1}{2\tau_{imp}} g_1^3. \tag{4}$$

Let us note several interesting limits for this equation. The $\tau_{imp} \to \infty$ is the clean superconductor limit, which was considered in Refs. 24 and 25. The $\tau_{imp} \to 0$ is the strong disorder limit, in which Eq. (4) leads to results equivalent to those obtained by the Usadel equations[16]. Finally, $\Delta \to 0$ is the normal metal limit where non trivial (proximity) solutions follow from superconducting boundary conditions.

The bulk superconducting energy Δ_0 is a convenient energy scale for the system. Even in a normal metal, where $\Delta = 0$, non-trivial solutions can appear because of proximity with a superconductor. In this case we can still use Δ_0, the bulk gap parameter value in the neighboring superconductor as a convenient energy scale. To streamline the notation we denote the coefficient from Eq. (4) by $\alpha_s = \omega^2 + \Delta^2 + C_s/(4\tau_{imp})$, and normalize C_s and α_s by the superconducting energy Δ_0, to get $\tilde{C}_s = C_s/\Delta_0$ and $\tilde{\alpha}_s = \alpha_s/\Delta_0^2$. We also introduce dimensionless coordinate $\tilde{x} = x/\xi_0$ (where $\xi_0 \equiv v_F/\Delta_0$ is the superconducting coherence length), and dimensionless disorder strength $\beta = 1/(2\Delta_0\tau_{imp})$. With these substitutions we can write Eq. (4) as

$$\partial_{\tilde{x}}^2 g_1 = 4\tilde{\alpha}_s g_1 - 2\beta^2 g_1^3. \tag{5}$$

We can solve Eq. (5) without *explicit* reference to the other components of $\hat{g}$ (they do appear through the boundary conditions, of course). The solution is implicitly given as an integral:

$$\int_{g_1(\tilde{x}_1)}^{g_1(\tilde{x}_2)} \frac{\mathrm{d}g_1}{\pm\left[4\tilde{\alpha}_s g_1^2 - \beta^2 g_1^4 + 2\tilde{E}_s\right]^{1/2}} = \zeta\tilde{x}_2 - \zeta\tilde{x}_1. \tag{6}$$

Here, $\tilde{E}_s$ is a constant of integration (in itself a function of C_s), about which we will have more to say in Sec. IV. Note that the Fermi index $\zeta = \pm 1$ appears on the right side of Eq. (6), therefore the function g_1 is manifestly odd in momentum. We determine the plus/minus sign in front of the integrand by demanding consistency with the boundary conditions and the integration path so that the signs of both sides in Eq. (6) match. We will present an intuitive way to understand this solution in Sec. IV and show that only monotonic solutions are physically acceptable. For a solution that starts from $\tilde{x} = 0$, it is convenient to recast the integral in Eq. (6) in terms of the inverse elliptic function sn^{-1}, which leads to

$$\mathrm{sn}^{-1}\left(\frac{g_1(\tilde{x}')}{(\rho_s^+)^{1/2}}\middle|\frac{\rho_s^+}{\rho_s^-}\right)\Bigg|_0^{\tilde{x}} = \pm\zeta\beta\tilde{x}[-\rho_s^-]^{1/2}, \tag{7a}$$

$$\rho_s^\pm = \frac{1}{\beta^2}\left(2\alpha_s \pm \left[4\alpha_s^2 + 2\tilde{E}_s\beta^2\right]^{1/2}\right). \tag{7b}$$

where $\tilde{x}'$ is a dummy variable.

Once we have $g_1(x)$, we can straightforwardly obtain the other components by using the constant of integration C_s and the system in Eq. (2), to get

$$g_2(x) = \frac{\tilde{\Delta}\left(\tilde{C}_s - \beta g_1^2(x)\right) - \tilde{\omega}\zeta\partial_{\tilde{x}} g_1(x)}{2\left(\tilde{\omega}^2 + \tilde{\Delta}^2\right)}, \tag{8a}$$

$$g_3(x) = \frac{\tilde{\omega}\left(\tilde{C}_s - \beta g_1^2(x)\right) + \zeta\tilde{\Delta}\partial_{\tilde{x}} g_1(x)}{2\left(\tilde{\omega}^2 + \tilde{\Delta}^2\right)}. \tag{8b}$$

III. THE P-WAVE CASE

In the case of a p-wave wire we consider spinless fermions. As in the previous section, we decompose $\hat{g}$

using the Pauli matrices $\hat{\tau}_i$. The order parameter can be written as $\zeta\Delta_0 i\tau_2$, and we again assume that Δ is a constant in space. The difference from the s-wave case arises from the fact that now g_2 is p-wave, and g_1 contains the secondary s-wave (odd-frequency) correlations[27–29].

The components of $\hat{g}$ again obey three coupled differential equations, which differ from the s-wave case, due to the Fermi surface averaging in the last term of Eq. (1). In the p-wave case the order parameter has a p-wave symmetry, therefore we get $\langle g_1\rangle = g_1$, $\langle g_2\rangle = 0$. Note that $\langle g_3\rangle = g_3$ applies (particle-hole correlations are s-wave-like). With these we have

$$\zeta v_F \partial_x g_1 = -2\omega g_2 + 2\zeta\Delta g_3 - \frac{1}{\tau_{imp}} g_2 g_3, \qquad (9a)$$

$$\zeta v_F \partial_x g_2 = -2\omega g_1, \qquad (9b)$$

$$\zeta v_F \partial_x g_3 = 2\zeta\Delta g_1 - \frac{1}{\tau_{imp}} g_1 g_2. \qquad (9c)$$

In the clean case, these equations are linear and easily solved[21,24,25]. Impurities introduce nonlinear coupling, proportional to $1/\tau_{imp}$. Nevertheless, as we demonstrate, these equations can be treated analytically. The next several steps closely follow the discussion in the preceding section. We have again identified a constant C_p obeying $\partial_x C_p = 0$. It is given by

$$C_p = -g_2^2/(2\tau_{imp}) + 2\zeta\Delta g_2 + 2\omega g_3. \qquad (10)$$

Using it we can derive from the system in Eqs. (9) a single second-order equation for g_2 :

$$v_F^2 \partial_x^2 g_2 = -2\zeta\Delta C_p + 4\alpha_p g_2 - \frac{3\zeta\Delta}{\tau_{imp}} g_2^2 + \frac{g_2^3}{2\tau_{imp}^2}, \qquad (11)$$

where for convenience we have introduced $\alpha_p = \omega^2 + \Delta^2 + C_p/(4\tau_{imp})$. Notice the difference with Eq. (4), which is for g_1.

Again, we use the energy scale Δ_0 (see Sec. II for more explanation) to introduce normalized coordinate $\tilde{x} = x/\xi_0$ (where $\xi_0 \equiv v_F/\Delta_0$), dimensionless disorder strength $\beta = 1/(2\Delta_0\tau_{imp})$, and normalize C_p and α_p as $\tilde{C}_p = C_p/\Delta_0$ and $\tilde{\alpha}_p = \alpha_p/\Delta_0^2$. With these substitutions Eq. (11) becomes

$$\partial_{\tilde{x}}^2 g_2 = -2\zeta\tilde{\Delta}\tilde{C}_p + 4\tilde{\alpha}_p g_2 - 6\zeta\beta\tilde{\Delta} g_2^2 + 2\beta^2 g_2^3. \qquad (12)$$

Now we integrate the equation Eq. (12), which can be done without any explicit reference to the other two components:

$$\int_{g_2(\tilde{x}_1)}^{g_2(\tilde{x}_2)} \frac{\mathrm{d}g_2}{\left[-4\zeta\tilde{\Delta}\tilde{C}_p g_2 + 4\tilde{\alpha}_p g_2^2 - 4\zeta\tilde{\Delta} g_2^3 + \beta^2 g_2^4 + 2\tilde{E}_p\right]^{1/2}} = \pm\zeta(\tilde{x}_2 - \tilde{x}_1) \qquad (13)$$

The Fermi momentum appears on the right hand side of equation Eq. (13) and g_2 is odd in momentum, as it should. We determine the plus/minus sign of the integral in Eq. (13) in order to be consistent with the boundary conditions and the integration path.

In this paper, we are interested in the behavior of the solution in a disordered normal metal next to a superconductor, so we consider the special case $\Delta = 0$, and recast the integral in Eq. (13) in terms of the inverse elliptic function sn^{-1} to get Eq. (14):

$$\mathrm{sn}^{-1}\left(\frac{g_2(\tilde{x}')}{(\rho_p^+)^{1/2}}\middle|\frac{\rho_p^+}{\rho_p^-}\right)\Bigg|_0^{\tilde{x}} = \pm\frac{\zeta\beta\tilde{x}}{\xi_0}[\rho_p^-]^{1/2}, \qquad (14a)$$

$$\rho_p^\pm = \frac{1}{\beta^2}\left(-2\alpha_p \pm \left[4\alpha_p^2 - 2\tilde{E}_p\beta^2\right]^{1/2}\right). \qquad (14b)$$

Once we have $g_2(x)$, we can obtain $g_1(x)$ and $g_3(x)$ by using the constant of integration C_p and the system in Eq. (9), to get

$$g_1(x) = \frac{-\zeta\partial_{\tilde{x}} g_2(x)}{2\tilde{\omega}}, \qquad (15a)$$

$$g_3(x) = \frac{\tilde{C}_p + \beta g_2(x)^2 - 2\zeta\tilde{\Delta} g_2(x)}{2\tilde{\omega}}. \qquad (15b)$$

IV. CLASSICAL PARTICLE ANALOGY

There is a surprising but intuitive way to understand the results from the previous two sections. We can think of Eq. 6 as an equation of motion of a classical particle with coordinate g_1, in an external force field. In this interpretation the normalized position $\zeta\tilde{x}$ takes the role of the dynamical time of this classical particle. The Hamiltonian of the classical particle is given by the following equation:

$$H_s[g_1] = \frac{1}{2}(\partial_{\tilde{x}} g_1)^2 - 2\tilde{\alpha}_s g_1^2 + \frac{\beta^2}{2} g_1^4. \qquad (16)$$

This Hamiltonian describes a particle in a double well potential $V_s[g_1] = -2\tilde{\alpha}_s g_1^2 + \beta^2 g_1^4/2$, as shown in Fig. 1. We denote the conserved energy of this Hamiltonian as $\tilde{E}_s$. We can furnish the solution to the "equation of motion" by inverting the integral in equation Eq.(6) that sums up to the elapsed time $\zeta\tilde{x}_2 - \zeta\tilde{x}_1$ between initial and final coordinates $g_1(\tilde{x}_1)$ and $g_2(\tilde{x}_2)$, respectively.

The double well potential $V_s[g_1]$, allows non-monotonic solutions. However, the classical turning points of this potential scale as $\pm(\omega\tau_{imp})$ at high frequency, and for both $\omega \to \infty$ or $\tau_{imp} \to \infty$ the non-monotonic motion has unbounded amplitude, hence these solutions are not physical. Therefore we will only consider the monotonic solutions. If we denote the poles of the integrand as $\rho_s^\pm$ then we can conveniently write the integral in Eq. (6) with monotonic integration path that starts from the point $g_1(\tilde{x} = 0)$, in terms of the inverse Jacobi elliptic function sn^{-1} as in equation Eq. (7).

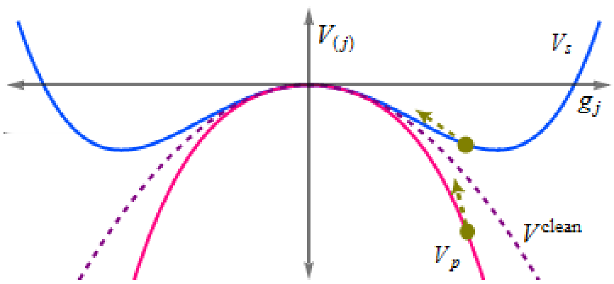

FIG. 1. The potential landscape of a classical particle with motion describing the Green's function, for a normal metallic segment, in contact with a superconductor. Depending on the superconductor (s or p-wave) potential is either V_s or V_p. In the clean limit both converge to V^{clean}.

In a similar manner, we can interpret Eq. (12) as the equation of motion of a classical particle with coordinate g_2, moving in an external potential. The Hamiltonian of this classical particle is given in Eq. (17)

$$H_p[g_2] = \frac{1}{2}(\partial_{\tilde{x}} g_2)^2 + 2\zeta\tilde{\Delta}\tilde{C}_p g_2 + 2\tilde{\alpha}_p g_2^2 - 2\zeta\tilde{\Delta} g_2^3 + \frac{\beta^2}{2} g_2^4. \tag{17}$$

The Hamiltonian given by equation Eq. (17) describes the particle in a double well potential $V_p[g_2] = 2\zeta\tilde{\Delta}\tilde{C}_p g_2 + 2\tilde{\alpha}_p g_2^2 - 2\zeta\tilde{\Delta} g_2^3 + \beta^2 g_2^4/2$. We denote the conserved energy of this Hamiltonian as $\tilde{E}_p$. We can again find the solution to the "equation of motion" by inverting the integral in equation Eq.(6) that sums up to the elapsed time $\zeta\tilde{x}_2 - \zeta\tilde{x}_1$ between initial and final coordinates $g_2(\tilde{x}_1)$ and $g_2(\tilde{x}_2)$, respectively.

In the special case of interest, where we are solving the equations in a disordered metal, $\Delta = 0$, therefore the potential $V_p[g_2]$, shown in Fig. 1, permits only monotonic solutions (given in Eq. (14)).

V. P-WAVE WIRE WITH NORMAL SEGMENT

We now proceed to study the leakage of superconductivity in a metallic wire. We consider an infinite wire extending along the x-axis with two segments that meet at $x = 0$. The infinite segment on the left ($x < 0$) is made of clean p-wave superconductor with order parameter $\zeta\Delta_0$. The segment on the right ($x > 0$) is made of a diffusive normal metal (the order parameter is zero)[30].

We want a solution that for $x \to -\infty$ reproduces the mean field result for a uniform clean p-wave superconductor. Introducing the parameter B and the dimensionless variables $\tilde{\Omega} = \Omega/\Delta_0$, $\tilde{\omega} = \omega/\Delta_0$, we can write such a solution [21,31,34]:

$$g_1(x) = (1/\tilde{\omega})[1 - \tilde{\Omega}B]\exp(2\tilde{\Omega}x/\xi_0), \tag{18a}$$

$$g_2(x) = \zeta(1/\tilde{\Omega})\left(1 - [1 - \tilde{\Omega}B]\exp(2\tilde{\Omega}x/\xi_0)\right), \tag{18b}$$

$$g_3(x) = \left\{[1 - \tilde{\Omega}B]/(\tilde{\Omega}\tilde{\omega})\right\}\exp(2\tilde{\Omega}x/\xi_0) + \tilde{\omega}/\tilde{\Omega}. \tag{18c}$$

B has to be determined from the boundary conditions at the junction ($x = 0$). For simplicity, we consider the case of perfectly transparent boundary, which guarantees the continuity of the Green's functions at the junction [32]. (Note that Eqs. (18) were derived under the assumption that the order parameter is constant in the clean p-wave superconductor. For the purpose of comparison, we describe the self-consistent solutions for a clean, *intrinsic*, p-wave superconductor in the appendix.)

Now we consider the diffuse normal segment with infinite length. Then, for $x \to \infty$ we have $g_1 \to 0$, $g_2 \to 0$ and $g_3 \to \mathrm{sgn}(\omega)$, and using the constant of integration $\tilde{C}_p(x = 0) = \tilde{C}_p(x \to \infty) = 2|\tilde{\omega}|$ we get a quadratic equation, with one of the two solutions given as:

$$B = \frac{1}{\beta}\left[-1 + \sqrt{1 + 2\beta(\tilde{\Omega} - \tilde{\omega})}\right]. \tag{19}$$

and we discard the other solution because it leads to a non-monotonic solution. We can understand intuitively the behavior of g_2 by invoking the classical analogy. The particle in potential V_p starts at "position" $g_2(0) = \zeta B$, with velocity $\partial_{\tilde{x}} g_2(0) = -2\tilde{\omega}\zeta g_1(0) = -2\zeta(1 - \tilde{\Omega}B)$, and moves towards its unstable equilibrium point $g_1(+\infty) = 0$, gradually slowing down until $\partial_{\tilde{x}} g_2(+\infty) = 0$, from which we deduce $\tilde{E}_p = 0$. Indeed, it takes infinite amount of time for the particle to reach the point $g_2 = 0$, a fact we see from the diverging integral in Eq. (13) for $\tilde{E}_p = 0$, as $g_2 \to 0$.

For $\tilde{E}_p = 0$ the elliptic integral leads to inverse hyperbolic functions, and defining the dimensionless constant $\kappa = [1 + \beta^2 B^2/(4\tilde{\alpha}_p)]^{1/2}$, we can write the solution for g_2:

$$g_2(x) = \frac{\zeta B}{\cosh(x/\xi') + \kappa\sinh(x/\xi')}. \tag{20}$$

Here $\xi' = \xi_0/(2\tilde{\alpha}_p^{1/2})$ gives the effective decay length of the solution (at $T = 0$). In physical units it is

$$\xi' = \frac{v_F}{\sqrt{4\omega^2 + 2|\omega/\tau_{imp}|}}. \tag{21}$$

In the dirty limit we have $\xi' = \sqrt{D/|\omega|}$, where D is the diffusion coefficient. Finally, in the clean limit g_2 converges to $\zeta B\exp(-2|\tilde{\omega}|x/\xi_0)$, as expected [21].

The other two components of the Green's function can be derived from g_2 using $\tilde{C}_p$ and the Eilenberger equations: $g_1 = -\zeta\xi_0\partial_x g_2/(2\tilde{\omega})$ and $g_3 = \mathrm{sgn}(\tilde{\omega}) + \beta g_2^2/(2\tilde{\omega})$. As expected, impurities suppress g_2 relative to g_1. However, they both decay in the normal segment over the *same* length scale, given by Eq. (21). This decay is long-range, and furthermore, with exactly the same length scale obtained for the case of s-wave order parameter[24,25]. Thus, the naïve expectation of strong suppression of the p-wave correlations is misleading in this case. This is one of the main points of our paper[33], and it is also supported by the fact that the same decay length scale appears also in the case of an s-wave superconductor with magnetic disorder[26], which is known to be analogous in some ways to a p-wave superconductor with potential disorder.

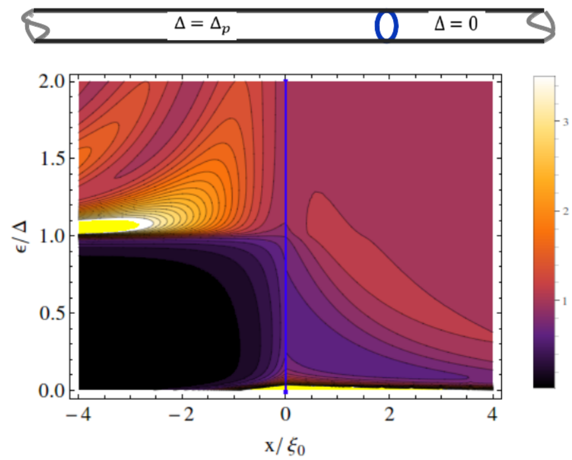

FIG. 2. Contour plot of the DOS of an infinite wire. There is moderate disorder ($\beta = 1$) in the normal segment ($x > 0$). The solid yellow marks the regions that are beyond the plot range (where $N/N_0 > 3.5$). Notice the zero-energy peak in the normal segment.

We can now obtain the DOS of the system from $\mathrm{Re}[g_3(\omega \to -i\epsilon + \delta)]$[21]. On Fig. 2 we show it for a system with moderate disorder. Several things are apparent from this plot. First, for low energies there is a significant decrease in the DOS of the normal segment, caused by the proximity effect; however, it is not a real gap, since the DOS stays finite. This decrease is entirely due to the impurities, which "trap" the superconducting correlations close to the boundary (in the clean case the DOS is constant for $x > 0$ [21]). The impurity-induced term in g_3 also has a divergence in the limit of small frequencies ($g_3 \sim 1/\omega$), which leads to an infinite peak in the DOS (see Fig. 3). This zero-energy peak has the same origin as the Majorana edge state (namely, the sign change in the order parameter[31,34,35]). From Eq. (20), we can see that the weight of the zero-energy peak has a power-law decay $\sim (1 + \beta B x/\xi_0)^{-2}$ into the metalic segment.

As a side note, in the case of an s-wave superconductor, the solution of Eq. (4) is $g_1 = \zeta A[\cosh(x/\xi') + \kappa_s \sinh(x/\xi')]^{-1}$, with A and κ_s that can be derived by matching the solutions at the junction. However, unlike the p-wave case, the g_1 component at the boundary is proportional to $\tilde{\omega}$. This dependence on $\tilde{\omega}$ changes the behavior of the DOS. From $g_3 = \mathrm{sgn}(\tilde{\omega}) - \beta/(2\tilde{\omega})g_1^2$, we

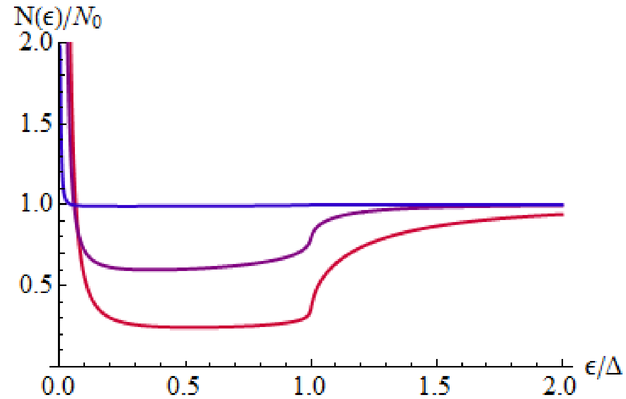

FIG. 3. DOS at the junction of infinite normal and superconducting segments. Three cases for the disorder in the normal segment are plotted: weak ($\beta = 0.1$, blue), moderate ($\beta = 1$, purple), and strong ($\beta = 10$, red). Notice the suppression of DOS with the increase of disorder strength.

can see that the low frequency limit is finite, and there is no zero energy peak in the s-wave case[36].

If the normal segment has finite length L, we impose the condition $g_2(L) = 0$ (the p-wave component is suppressed by boundary reflection). Then the solution follows immediately from Eq. 14 as $g_2(x) = \zeta(\rho_p^+)^{1/2}\mathrm{sn}[\beta(\rho_p^-)^{1/2}(x - L)/\xi_0]$, with elliptic parameter $m = \rho_p^+/\rho_p^-$. However, this expression has limited value, since B_L, which should be obtained from matching the two solutions for g_2 at $x = 0$, enters the expression through the parameters $\rho_p^\pm$, and is difficult to find. Fortunately, an approximate analytic form for B_L can be obtained. Numerical investigation suggests that B_L can be approximated by $B[1 - \exp(-2L/\lambda_B)]$, with $\lambda_B = B\xi_0$ (it controls how quickly B_L approaches to the infinite wire limit). Once we have B_L, we can write g_2 in a form that manifestly converges to that of the $L = \infty$ case[37]. To save space, we shorten the common argument of elliptic functions, $\beta|\rho_p^-|^{1/2}x/\xi_0$ as (.). The common elliptic parameter of the elliptic functions is $(\rho_p^- - \rho_p^+)/\rho_p^-$, and it lies in the interval $[0, 1]$. With these definition we get:

$$g_2(x) = \zeta \frac{B_L \mathrm{dn}(.) - \mathrm{sn}(.)\mathrm{cn}(.)\sqrt{|\rho_p^+| + B_L^2}\sqrt{1 + B_L^2/|\rho_p^-|}}{\mathrm{cn}^2(.) - (B_L^2/|\rho_p^-|)\mathrm{sn}^2(.)}. \tag{22}$$

We can again obtain the two other components from g_2 by using: $g_1 = -\zeta\xi_0\partial_x g_2/(2\tilde{\omega})$ and $g_3 = (\tilde{\alpha}_p - \tilde{\omega}^2)/(\beta\tilde{\omega}) + \beta g_2^2/(2\tilde{\omega})$. Figure 4 shows the components g_1, g_2, g_3 of the quasiclassical matrix Green's function $\hat{g}$, for varying disorder strengths, over a semi infinite wire with disordered section. As $L \to \infty$, the elliptic functions are replaced by their hyperbolic counterparts, and we recover Eq. 20. This convergence is exponential, so the wire is effectively infinite when $L/(B\xi_0) \gg 1$. Conversely, if $L/(B\xi_0) \ll 1$, $g_2(x)$ decays linearly in the normal metal. Again, it is the impurity-induced contribution to g_3 that is of most

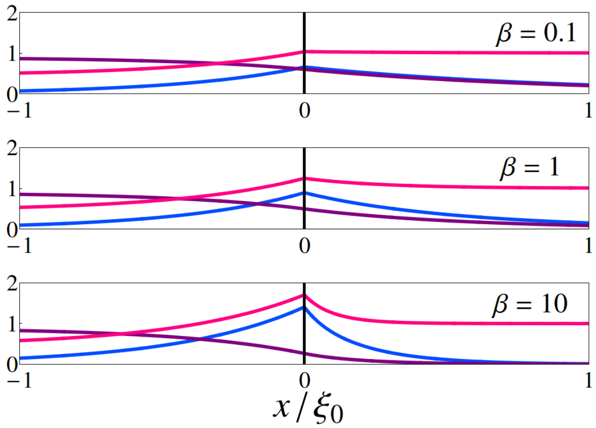

FIG. 4. Components of $\hat{g}$,(g_1: blue, g_2: purple, g_3: red) for a wire with infinite p-wave section and finite disordered section of length $L = 5\xi_0$. Top panel: weak disorder($\beta = 1/(2\tau_{imp}\Delta_0) = 0.1$). Middle panel: moderate disorder ($\beta = 1$). And bottom panel: strong disorder ($\beta = 10$). The Matsubara frequency is set to $\omega = \Delta_0/2$.

interest. After analytic continuation we can write the zero-energy limit as

$$g_3(x) = \frac{1}{\pi}\delta(\epsilon)\mathcal{M}(x). \tag{23}$$

Here, $\mathcal{M}(x)$ describes the x-dependent weight of the zero energy mode, and can be extracted from Eq. (22):

$$\mathcal{M}(x) = \frac{\alpha_p}{\beta} + \frac{\beta}{2}\left(\frac{B_L - \sqrt{\frac{\alpha_p}{2\beta^2}}\left(1+\frac{\beta^2 B^2}{2\alpha_p}\right)\sin(.)\cos(.)}{\cos^2(.) - \frac{\beta^2 B^2}{2\alpha_p}\sin^2(.)}\right)^2. \tag{24}$$

It is monotonically decreasing function, and its values at the ends of the wire are $\mathcal{M}(0) = 1 - B_L$ and $\mathcal{M}(L) = \mathcal{M}(0) - \beta B_L^2/2$ respectively. Figure 5 shows $\mathcal{M}(x)$ in the normal section with length $L = 5\xi_0$, for various disorder strengths. As can be seen, it becomes peaked closer to $x = 0$ as the disorder in the normal section increases. On the other hand, for weak disorder, $[\mathcal{M}(0) - \mathcal{M}(L)]/(L/\xi_0)$ is small, so the zero-energy peak is delocalized over the entire normal segment.

VI. CONCLUSION

We presented a quasiclassical description of a quasi-one-dimensional superconductor. The appropriate Eilenberger equations of the system were solved *exactly*. Surprisingly, we discovered that this problem can be mapped to a one-dimensional classical particle moving in an external potential. In view of the recent interest in superconducting heterostructures, we studied the proximity effects in a normal segment, attached to a clean p-wave wire. We discovered that despite the presence of impurities, the proximity-induced superconducting correlations are long-range. We also found that impurity scattering leads to the appearance of a delocalized zero-energy peak.

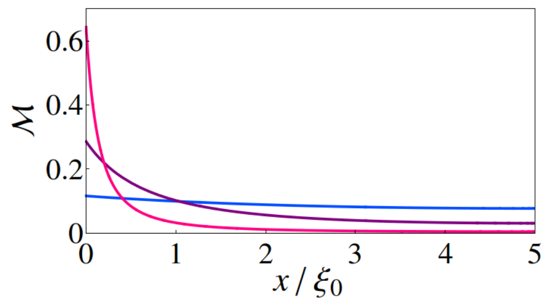

FIG. 5. The weight of the zero energy mode $\mathcal{M}(x)$ in a normal section with length $L = 5\xi_0$ for three disorder strengths (blue: $\beta = 0.1$, purple: $\beta = 1$, red: $\beta = 10$).

ACKNOWLEDGMENTS

We thank Dmitri Efimkin for pointing out to us Ref. 38. This research was supported by DOE-BES DESC0001911 (VG & VS), NSF-CAREER DMR-0847224 (ACK), and Simons Foundation.

Appendix: Self-consistent solutions of the Eilenberger Equations in a clean quasi 1-D superconductor

The Green's function solutions we presented in Eq. (18) are derived under the assumption that the order parameter is constant and equal to $\zeta\Delta_0$ in the clean segment of the wire. Indeed, a more accurate model should take into account the suppression of the order parameter near the junction with the dirty normal metal. However, the precise way to treat a proximity p-wave superconductor depends on the experimental details of the system and is beyond the scope of this work. Nevertheless, here, we present the self-consistent exact solution to the quasiclassical Green's function in a clean superconductor for both *intrinsic* s-wave and *intrinsic* p-wave cases. We also calculate how to match these solutions at the junction with a dirty metal for a comparison. We note that the self consistent treatment does not alter the form of the solution in Eq. (20) or the decay length scale Eq. (21). The only effect is the modification of the matching parameter in Eq. (19).

The calculations presented here are special cases of an approach developed to explain phase slips in clean superconducting wires (see Ref. 38 for more details).

1. Solution for the p-wave case

We neglect the τ_{imp}^{-1} terms in Eq. (9) to obtain equations for clean p-wave superconductor. We assume Δ is a function of x. We normalize the equations by introducing bulk value of the order parameter (far from the junction) Δ_0 as an energy scale. Then $\xi_0 = v_F/\Delta_0$ is the length scale and the normalized coordinate becomes $\tilde{x} = x/\xi_0$. Similarly, the normalized Matsubara frequency and the normalized order parameter read as $\tilde{\omega} = \omega/\Delta_0$ and $\tilde{\Delta}(\tilde{x}) = \Delta(x/\xi_0)/\Delta_0$ respectively. We also define $\Omega = \sqrt{\omega^2 + \Delta_0^2}$ and its normalized version $\tilde{\Omega} = \Omega/\Delta_0$.

The normalized equations read as:

$$\zeta\partial_{\tilde{x}} g_1 = -2\tilde{\omega} g_2 + 2\zeta\tilde{\Delta} g_3, \tag{A.1a}$$
$$\zeta\partial_{\tilde{x}} g_2 = -2\tilde{\omega} g_1, \tag{A.1b}$$
$$\zeta\partial_{\tilde{x}} g_3 = 2\zeta\tilde{\Delta} g_1. \tag{A.1c}$$

These equations are supplemented by the self consistency condition

$$\frac{\Delta}{\lambda} = \pi T \sum_{\omega_n} g_2(\omega_n, x) \tag{A.2}$$

The self consistent homogeneous solutions to these equations are known as:

$$g_1^{(0)} = 0, \quad g_2^{(0)} = \zeta/\tilde{\Omega}_n, \quad g_3^{(0)} = \tilde{\omega}_n/\tilde{\Omega}_n \tag{A.3}$$

Here, the subscript n counts the discrete Matsubara frequencies of the system. To obtain the self-consistent solutions, we observe that the following quantity is zero

$$\zeta\tilde{\Delta}\partial_{\tilde{x}} g_2 + \tilde{\omega}\partial_{\tilde{x}} g_3 = 0 \tag{A.4}$$

Let us make the following ansatz:

$$g_2(\tilde{x}) = \zeta\tilde{\Delta}(\tilde{x})/\tilde{\Omega} \tag{A.5}$$

Now, we can integrate equation Eq. A.4 as

$$S = \tilde{\Delta}^2 + 2\tilde{\omega}\tilde{\Omega} g_3 \tag{A.6}$$

We calculate the value of S using the values of the Green's function at the far end of the wire, since the solution converge to the equilibrium Green's function given in Eq. (A.3). This yields $S = 1 + 2\tilde{\omega}^2$.

Now, we obtain a closed equation in $\tilde{\Delta}$ by differentiating Eq. A.1b with respect to normalized position and replacing $g_3 = (S - \tilde{\Delta}^2)/(2\tilde{\omega}\tilde{\Omega})$. This yields:

$$\partial_{\tilde{x}}^2\tilde{\Delta} + 2\tilde{\Delta} - 2\tilde{\Delta}^3 = 0 \tag{A.7}$$

This differential equation can be interpreted as the equation of motion for a classical particle in a Ginzburg-Landau type potential given as $\tilde{\Delta}^2 - \tilde{\Delta}^4/2$. The solution that approaches the equilibrium value at minus infinity is easily obtained up to an unknown shift $\tilde{x}_0$:

$$\tilde{\Delta} = -\tanh(\tilde{x} - \tilde{x}_0) \tag{A.8}$$

We determine the solutions for the components of the Green's up to a shift $\tilde{x}_0$ in the position argument as:

$$g_1(\tilde{x}) = \frac{1}{2\tilde{\omega}\tilde{\Omega}}\frac{1}{\cosh(\tilde{x} - \tilde{x}_0)^2}, \tag{A.9a}$$
$$g_2(\tilde{x}) = \frac{-\zeta}{\tilde{\Omega}}\tanh(\tilde{x} - \tilde{x}_0), \tag{A.9b}$$
$$g_3(\tilde{x}) = \frac{1}{2\tilde{\omega}\tilde{\Omega}}\frac{1}{\cosh(\tilde{x} - \tilde{x}_0)^2} + \frac{\tilde{\omega}}{\tilde{\Omega}} \tag{A.9c}$$

We determine the unknown parameter $\tilde{x}_0$ by enforcing the other boundary condition. In this problem we will parametrize this unknown in terms of the value of ζg_2 at the junction point $B_{sc} = \zeta g_2(0)$. Therefore we write $\tilde{\Omega} B_{sc} = \tanh(\tilde{x}_0)$.

Here we write the values of the Green's function components at the junction point in terms of B_{sc}.

$$g_1(0) = \frac{1}{2\tilde{\omega}\tilde{\Omega}}\left[1 - (\tilde{\Omega} B_{sc})^2\right], \tag{A.10a}$$
$$g_2(0) = \zeta B_{sc}, \tag{A.10b}$$
$$g_3(0) = \frac{1}{2\tilde{\omega}\tilde{\Omega}}\left[1 - (\tilde{\Omega} B_{sc})^2\right] + \frac{\tilde{\omega}}{\tilde{\Omega}} \tag{A.10c}$$

2. Matching the solutions at $x = 0$

To determine B_{sc}, the self-consistent value of B in Eq. (20), we evaluate the constant in Eq. (10) at different points as $C_p(0) = C_p(+\infty) = 2|\tilde{\omega}|$ by using (A.10c), which yields a quadratic equation with solution:

$$B_{sc} = \frac{\tilde{\Omega} - |\tilde{\omega}|}{\sqrt{\tilde{\Omega}(\tilde{\Omega} + \beta)}} \tag{A.11}$$

The negative root of the quadratic does not satisfy the condition $g_2\partial_{\tilde{x}} g_2 < 0$ that the monotonic function g_2, approaching zero at infinity, has to satisfy. Comparing with Eq. (19), we see that the self-consistent solution to the g_2 is suppressed by a factor of $\sim 1/\tilde{\Omega}$.

3. Solution for the s-wave case

It turns out that all the arguments for the p-wave case apply here, except for that , the p-wave component is g_1 rather than g_2. Therefore the self consistent solution to the Green's function in an s-wave clean superconductor is:

$$g_1(\tilde{x}) = \frac{\zeta}{2\tilde{\omega}\tilde{\Omega}} \frac{1}{\cosh(\tilde{x}-\tilde{x}_0)^2}, \tag{A.12a}$$

$$g_2(\tilde{x}) = \frac{-1}{\tilde{\Omega}} \tanh(\tilde{x}-\tilde{x}_0), \tag{A.12b}$$

$$g_3(\tilde{x}) = \frac{1}{2\tilde{\omega}\tilde{\Omega}} \frac{1}{\cosh(\tilde{x}-\tilde{x}_0)^2} + \frac{\tilde{\omega}}{\tilde{\Omega}} \tag{A.12c}$$

---

[1] L. Fu and C.L. Kane, Phys. Rev. Lett. **100**, 096407 (2008).

[2] J. D. Sau, R. M. Lutchyn, S. Tewari, and S. Das Sarma, Phys. Rev. Lett. **104**, 040502 (2010).

[3] R.M. Lutchyn, J.D. Sau, and S. Das Sarma, Phys. Rev. Lett. **105**, 077001 (2010).

[4] J. Alicea, Phys. Rev. B **81**, 125318 (2010).

[5] Y. Oreg, G. Refael, and F. von Oppen, Phys. Rev. Lett. **105**, 177002 (2010).

[6] M. Wimmer, A. R. Akhmerov, M. V. Medvedyeva, J. Tworzydo, C. W. J. Beenakker, Phys. Rev. Lett. **105**, 046803 (2010).

[7] V. Mourik, K. Zuo, S. Frolov, S. Plissard, E. Bakkers, and L. Kouwenhoven, Science **336**, 1003 (2012).

[8] M.T. Deng, C.L. Yu, G.Y. Huang, M. Larsson, P. Caroff, and H.Q. Xu, Nano Lett. **12**, 6414 (2012).

[9] A. Das, Y. Ronen, Y. Most, Y. Oreg, M. Heiblum, and H. Shtrikman, Nat. Phys. 8, 887 (2012).

[10] P.W. Brouwer, M. Duckheim, A. Romito, and F. von Oppen, Phys. Rev. B **84**, 144526 (2011).

[11] A. R. Akhmerov, J. P. Dahlhaus, F. Hassler, M. Wimmer, and C. W. J. Beenakker, Phys. Rev. Lett. **106**, 057001 (2011).

[12] W. DeGottardi, D. Sen, and S. Vishveshwara, New J. Phys. **13**, 065028 (2011).

[13] A. M. Lobos, R. M. Lutchyn, and S. Das Sarma, Phys. Rev. Lett. **109**, 146403 (2012).

[14] P. W. Anderson, J. Phys. Chem. Solids **11**, **26** (1959).

[15] K. L. Usadel, Phys. Rev. Lett. **25**, 507 (1970).

[16] F. S. Bergeret, A. F. Volkov, and K. B. Efetov, Rev. Mod. Phys. **77**, 1321 (2005), and references therein.

[17] G. Eilenberger, Z. Phys. **214**, 195 (1968).

[18] See, for example, N. B. Kopnin, *Theory of Nonequilibrium Superconductivity* (Clarendon Press, Oxford 2001).

[19] P. Neven, D. Bagrets, and A. Altland, New J. Phys. **15**, 055019 (2013).

[20] S. Abay, D. Persson, H. Nilsson, F. Wu, H.Q. Xu, M. Fogelström, V. Shumeiko, and P. Delsing, Phys. Rev. B **89**, 214508 (2014).

[21] V. Stanev, and V. Galitski, Phys. Rev. B **89**, 174521 (2014).

[22] H.-Y. Hui, J. D. Sau, and S. Das Sarma, Phys. Rev. B **90**, 064516 (2014).

[23] For a recent comparison between quasiclassical and fully microscopic calculation of the same structure, see, for example, C. Reeg, and D. Maslov, Phys. Rev. B **90**, 024502 (2014).

[24] F.S.Bergeret, A.F. Volkov, K.B.Efetov, Phys. Rev. B **65**, 134505 (2002).

[25] I. Baladié and A. Buzdin, Phys. Rev. B **64**, 224514 (2001).

[26] F.S. Bergeret, A.F. Volkov, K.B. Efetov, Phys. Rev. B **75**, 184510 (2007).

[27] A. Golubov, Y. Tanaka, Y. Asano, and Y. Tanuma, J. Phys.: Condens. Matter **21**, 164208 (2009)

[28] Y. Tanaka, M. Sato, and N. Nagaosa, J. Phys. Soc. Jpn. **81**, 011013 (2012), and references therein.

[29] Note that the odd-frequency correlations are different from the odd-frequency order parameter, which was originally proposed for ^{3}He by Berezinskii (V. L. Berezinskii, JETP Lett. **20**, 287 (1975)), and was later studied in the context of curpates (A. Balatsky, and E. Abrahams, Phys. Rev. B **45**, 13125 (1992), A. Balatsky, E. Abrahams, D. J. Scalapino, and J. R. Schrieffer, Phys. Rev. B **52**, 1271 (1995)).

[30] We are, in fact, considering a quasi-one-dimensional system, with several conducting channels, rather than a truly one-dimensional wire, which would be in an insulating state even for infinitesimal disorder strength.

[31] M. Matsumoto and M. Sigrist, J. Phys. Soc. Jpn. **68**, 994 (1999).

[32] More realistic modeling of the boundary requires more complicated boundary conditions: A. V. Zaitsev, Zh. Eksp. Teor. Fiz. 86, 1742 (1983) [Sov. Phys. JETP **59**, 1015 (1984)], and G. Kieselmann, Phys. Rev. B **35**, 6762 (1987).

[33] Also, note that the order parameter amplitude Δ_0 appears only in the boundary conditions at $x = 0$. Thus, even a complete self-consistent treatment of the superconducting segment would not change the decay length, only the overall prefactor. See Appendix for more details.

[34] M. Matsumoto, M. Koga, and H. Kusunose, J. Phys. Soc. Jpn. **82**, 034708 (2013).

[35] See also A. Fauchre, W. Belzig, and G. Blatter, Phys. Rev. Lett. **82**, 3336 (1999).

[36] Analogous calculation in the s-wave case leads not to a peak, but linear suppression of DOS at low energies. The overall DOS profiles are very similar to those obtained earlier numerically (see, e.g., W. Belzig, C. Bruder, and G. Schon, Phys. Rev. B, **54**, 9443 (1996)).

[37] I. S. Gradshteyn, I. M. Ryzhik, *Table of integrals, tables and products*, Alan Jeffrey and Daniel Zwillinger (eds.) Seventh edition (Academic 2007), Section 8.1

[38] A. Zharov, A. Lopatin, A. E. Koshelev, and V. M. Vinokur, Phys. Rev. Lett. **98**, 197005 (2007).